No evidence for Evans' holes in the A, B, C vibrational structure of potassium dihydrogen arsenate

John Tomkinson,[1,a)] Stewart F. Parker,[1,b)] and David Lennon[2,c)]
[1]*The Rutherford Appleton Laboratory, Science and Technology Facilities Council, Harwell Science and Innovation Campus, Oxfordshire OX11 0QX, United Kingdom*
[2]*Department of Chemistry, Joseph Black Building, University of Glasgow, Glasgow G12 8QQ, United Kingdom*

(Received 16 April 2010; accepted 7 June 2010; published online xx xx xxxx)

We have used inelastic neutron scattering (INS) spectroscopy to study the "A, B, C" region of the hydrogen bond in potassium dihydrogen arsenate. The broad spectral feature observed in infrared spectroscopy is shown to be associated with a ridge of constant intensity in the INS, which follows the recoil line for a unit-mass particle. The onset energy of the ridge is unclear but, we believe, is associated with the optical "C" feature at 1610 cm^{-1}, and which we assign to ν(O–H). The "B" and "A" optical bands were both demonstrated to be two-quantum events and are, thus, not associated with the fundamental ν(O–H). They are readily assigned to the harmonic overtone δ(OH)(0-2) and the combination γ(OH)(0-1)+δ(OH)(0-1), which both sit astride the ridge and there is no evidence for Evans' holes. The other overtone, γ(OH)(0-2), has been assigned to a very weak feature, observed for the first time at 1900 cm^{-1}. A simple model was used to describe the intensity distributions. © *2010 American Institute of Physics*. [doi:10.1063/1.3457788]

I. INTRODUCTION

In the infrared vibrational spectroscopy of hydrogen bonds, here O–H···O, the great strength and width of the high frequency stretching vibration, ν(O–H), has always been of interest. Its intense infrared response serves not only as a clear indicator of the presence of a H-bond but the energy of the transition is closely linked to the strength of the H-bond.[1] The infrared ν(O–H) band is often heavily structured and the causes of this have been a rich topic of research for several decades, although recent work now favors one particular model.[2] In one category of H-bond, where the center of the broad ν(O–H) band is about 2000 cm^{-1}, the vibrational structure is especially simple; the band is split into three subbands, "A," "B," and "C" (named from high to low energies). It was soon realized that this structure could be explained by two models, either an enhancement of intensity in the regions of the subbands, or of intensity loss in the two gaps between the bands, the A-to-B and B-to-C "windows."[3] The latter model could be explained in terms of narrow, usually, optically inactive modes interacting with the broad response of the ν(O–H) band and creating the so-called *Evans' holes*.[4] Indeed, the harmonic overtones of the deformation modes of the hydrogen bond (the out-of-plane γ(O–H)(0-2) and in-plane δ(O–H)(0-2) deformations, respectively) could fall at positions suitably close to the observed windows. Demonstrating which of the two models applies to a given spectrum has not proved straightforward because the problem is obscured by the presence of other effects, *inter alia* electrical anharmonicity.

Furthermore, the vibrational spectra of heterogeneous catalysts, where the presence of surface hydroxyl groups can markedly influence catalytic performance, have been discussed in terms of A, B, C bands. For example, the infrared spectra of H-surface complexes on deuterated H-ZSM5 and H-FeSil zeolites.[5] Similarly, the acidobasic properties of surface complexes of zeolites of various acidity have been probed using infrared spectroscopy interpreted through theoretical models.[6] In particular, that work highlighted the importance of determining the fundamental δ(OH) and γ(OH) deformation energies of surface –OH groups from the infrared spectra of the surface complexes. Unfortunately, the substrate modes of technical grade catalysts often limit the use of optical spectroscopy (in the case of alumina based catalysts bands below the "cut-off," ~1100 cm^{-1}, are inaccessible) and the δ and γ modes are normally obscured in zeoletic systems and metal oxide supported catalysts.[7] However, inelastic neutron scattering (INS) spectroscopy is ideally suited to the study of H-bonds, in general,[8] and the determination of both δ and γ in catalytic materials (at least for high surface area systems[9]). In this technique the hydrogen atom eigenvectors are observed directly and the enhancement of transition strengths by electrical anharmonicity plays no role.[10] Taken together there is a strong complementarity between the infrared and INS techniques when used to characterize technical grade catalysts. It is, as well, then that the true nature of the A, B, C bands be fully understood so that they can be suitably exploited in other fields of study.

Therefore, we have undertaken the study of one particular A, B, C system, potassium dihydrogen arsenate, KH_2AsO_4 (KDAs). This system has already seen some pre-

[a)]Author to whom correspondence should be addressed. Electronic mail: john.tomkinson@stfc.ac.uk. Tel.: 00-44-1235-44-6686. FAX: 00-44-1235-44-5720.
[b)]Electronic mail: stewart.parker@stfc.ac.uk. Tel.: 00-44-1235-44-6182. FAX: 00-44-1235-44-5720.
[c)]Electronic mail: davidle@chem.gla.ac.uk. Tel.: 00-44-1413-30-4372. FAX: 00-44-1413-30-4888.

liminary INS work,[11] and was studied using optical spectroscopy to draw the conclusion that the A-to-B gap is best described as a window, as might also be the other gap.[12] Here we shall follow the variation of the INS intensities of the A, B, C bands as we vary the neutron momentum transferred. The crystallographic details of KDAs are given in Sec. II, the quantitative INS theory is outlined in Sec. III, the INS measurements in Sec. IV, data treatment in Sec. V, and the results are presented in Sec. VI and discussed in Sec. VII.

II. CRYSTALLOGRAPHIC DETAILS

The room temperature crystal structure of KDAs, $I\bar{4}2d(D_{2d}^{12})$ $Z=1$,[13] implies the equal sharing of the hydrogen atoms across two sites. Below its critical temperature, at $T_c=97$ K, the hydrogen atoms are randomly associated with specific oxygen atoms and the system becomes locally ordered into ferroelectric domains, $Fdd2(D_{2v}^{19})$. The arsenate tetrahedra are held together by hydrogen bonds that link their corners in sheets, in the a, b plane, and the short tetragonal axis lies along the unique direction c. Unfortunately, no detailed neutron diffraction work is reported on this arsenate, so the atomic displacement parameters (ADPs) (Ref. 14) of the hydrogen atom are unknown. However, ADP values are available for the hydrogen atom in the structurally isomorphous (and spectroscopically similar) potassium dihydrogen phosphate.[15] We can compare the ADP values of the oxygen in this phosphate, $^{\mathrm{Tr}}\mathbf{U}(\mathrm{O})$, to those of the oxygen in KDAs (both at T_c+5 K); then $^{\mathrm{Tr}}\mathbf{U}(\mathrm{O})_{\mathrm{P}}:{}^{\mathrm{Tr}}\mathbf{U}(\mathrm{O})_{\mathrm{As}}::0.026\,13:0.0282$. They are in reasonable agreement and, so, we use the KDP value of $^{\mathrm{Tr}}\mathbf{U}(\mathrm{H})$, 0.054 42 Å^2 (at T_c-20 K) as an estimate for that of the KDA hydrogen atom below its T_c. Some correction should be made for the differences of temperature, 77 K for the diffraction value and 20 K in this work, but we can accept $^{\mathrm{Tr}}\mathbf{U}(\mathrm{H})=0.054\,42$ Å^2 as the maximal value for purposes of broad comparison.

III. THEORY

The intensity observed, S (arbitrary units), at momentum transfer, Q(Å^{-1}) and energy transfer, ω(cm^{-1}), is given by

$$S(Q,\omega)^{\nu}=I\Gamma, \tag{1}$$

where the observed intensity as a function of Q (the Q-profile) is $I(Q)$ and Γ is the full width at half height (FWHH) in ω. This intensity is related to the theoretical expressions,[10]

$$S(Q,\omega)^{\nu}|(0-1)=\mathrm{X}\frac{Q^2}{3}{}^{\mathrm{Tr}}(^{\nu}\mathbf{B})\exp(-Q^2\alpha^{\nu}),$$

$$\alpha^{\nu}=\frac{1}{5}\{{}^{\mathrm{Tr}}\mathbf{A}+2\ {}^{\nu}\mathbf{B}\}\quad \alpha^{\nu}\approx\frac{{}^{\mathrm{Tr}}\mathbf{A}}{3}, \tag{2}$$

where $^{\mathrm{Tr}}(^{\nu}\mathbf{B})$ is the trace of the mean square displacement tensor (Å^2) of the hydrogen bonded hydrogen atom in its vibrational mode ν, and the tensor $\mathbf{A}$ is defined below. For a harmonic vibration the components of its $\mathbf{B}$ tensor, oriented to its principle axes, are given by (for an oscillator mass, μ)

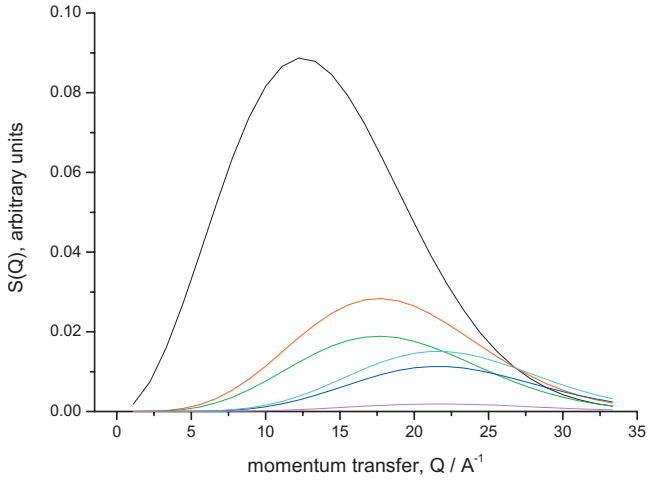

FIG. 1. The ideal shapes of the theoretical Q-profile curves according to Eq. (2) one-quantum transitions, (0-1) in black; Eqs. (4) and (5) two-quantum transitions, (0-2) in red, (0-1)(0-1′) in green; and three-quantum transitions, (0-3) in dark blue, (0-2)(0-1) in light blue, (0-1)(0-1′)(0-1″) in mauve. Here $^{\mathrm{Tr}}\mathbf{B}=0.004\,66$ Å^2 and $\alpha=0.0044$ Å^2.

$$^{\nu}\mathbf{B}=\begin{bmatrix} u_{\nu}^2 & & \\ & 0 & \\ & & 0 \end{bmatrix}\quad \text{where}\quad u_{\nu}^2=\frac{16.759}{\omega_{\nu}\mu_{\nu}}. \tag{3}$$

Only relative intensities have been measured, hence the arbitrariness of the S units, and the need for a scaling factor X (determined experimentally). Equation (2) refers to fundamental transitions and similar forms are known for first overtones and combination transitions, Eqs. (4) and (5), respectively,[10]

$$S(Q,\omega)^{\nu}|(0\text{-}2)$$

$$=\mathrm{X}\frac{Q^4}{30}\{{}^{\mathrm{Tr}}(^{\nu}\mathbf{B})\,{}^{\mathrm{Tr}}(^{\nu}\mathbf{B})+2\ {}^{\nu}\mathbf{B}:{}^{\nu}\mathbf{B}\}\exp(-Q^2\beta^{\nu})$$

$$\beta^{\nu}=\frac{1}{7}\{{}^{\mathrm{Tr}}\mathbf{A}+4\ {}^{\nu}\mathbf{B}\}, \tag{4}$$

$$S(Q,\omega)^{\nu}\begin{vmatrix}(0\text{-}1')(0\text{-}1)\\(0\text{-}1)(0\text{-}1')\end{vmatrix}$$

$$=\mathrm{X}\frac{Q^4}{15}\{{}^{\mathrm{Tr}}(^{\nu}\mathbf{B})\,{}^{\mathrm{Tr}}(^{\nu'}\mathbf{B})+(^{\nu}\mathbf{B}:{}^{\nu'}\mathbf{B})+(^{\nu'}\mathbf{B}:{}^{\nu}\mathbf{B})\}$$

$$\times\exp(-Q^2\beta^{\nu'\nu})$$

$$\beta^{\nu'\nu}=\frac{1}{7}\{{}^{\mathrm{Tr}}\mathbf{A}+2\ {}^{\nu'}\mathbf{B}+2\ {}^{\nu}\mathbf{B}\}. \tag{5}$$

The form of these curves is shown in Fig. 1. The observed data taken for given transitions can identify them as fundamentals by fitting to Eq. (2) and a unique parametrization is obtained. Unfortunately, it is very difficult to identify an event as specifically from a two-quantum transition by fitting alone. This is because the forms of higher order transitions [e.g., (0-3) or (0-2)(0-1)] can be made to reasonably fit two-quantum transitions but with different parameter values, see Fig. 2. Note, however, that data from fundamentals will not be well fitted to the forms of higher order transitions.

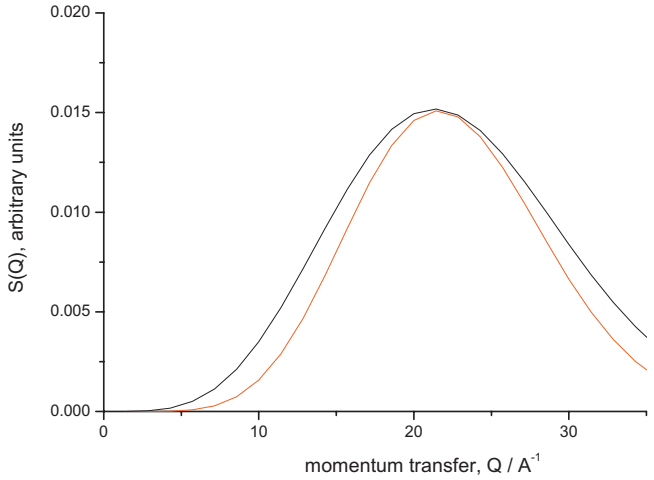

FIG. 2. The theoretical Q-profile curve of the two-quantum transition, (0-2), of Fig. 1 (α=0.0044), now in red, compared to a vertically scaled three-quantum transition (0-3), α=0.0064 Å^2.

The tensor **A** of the hydrogen atom is the sum of all its vibrational displacements and, in the absence of static disorder, is equivalent to its ADP, $^{\mathrm{Tr}}\mathbf{A} = {}^{\mathrm{Tr}}\mathbf{U}(\mathrm{H})$ (since they are usually referred to different axis systems only their traces are equal); **A** is given by

$$\mathbf{A} = \sum_{\nu} {}^{\nu}\mathbf{B} \quad \text{and} \quad \mathbf{A}_{\mathrm{tot}} = \sum_{\nu'} {}^{\nu'}\mathbf{B} + \sum_{\nu''} {}^{\nu''}\mathbf{B} \tag{6}$$

or

$$\mathbf{A}_{\mathrm{tot}} = \mathbf{A}_{\mathrm{external}} + \mathbf{A}_{\mathrm{internal}}.$$

Here $\mathbf{A}_{\mathrm{tot}}$ has been separated into its conventional molecular components, internal (high energy) and external (low energy). Where the ν' are the low energy modes (say below 500 cm^{-1}) and ν'' are the high energy modes (say above 1000 cm^{-1}), we also have

$$\mathbf{A}_{\mathrm{tot}} = \begin{bmatrix} \mathbf{A}_{11} & & \\ & \mathbf{A}_{22} & \\ & & \mathbf{A}_{33} \end{bmatrix}. \tag{7}$$

We shall find the logarithmic forms of Eqs. (2) and (4) useful,

$$\ln\left(\frac{S}{Q^2}\right) = \ln\left(\frac{\mathrm{X}}{3}{}^{\mathrm{Tr}}({}^{\nu}\mathbf{B})\right) - Q^2\alpha^{\nu}, \tag{8}$$

$$\ln\left(\frac{S}{Q^4}\right) = \ln\left(\frac{\mathrm{X}}{30}\{{}^{\mathrm{Tr}}({}^{\nu}\mathbf{B})\,{}^{\mathrm{Tr}}({}^{\nu}\mathbf{B}) + 2\,{}^{\nu}\mathbf{B}:{}^{\nu}\mathbf{B}\}\right) - Q^2\beta^{\nu}. \tag{9}$$

Or, generally, with n=2 or 4 and $\theta=\alpha$ or β,

$$\ln\left(\frac{I(Q)\Gamma}{Q^n}\right) = \ln({}^{\nu}\varphi) - Q^2\theta^{\nu}, \tag{10}$$

where α, β, and φ are the parameters fitted to the experimental results, $I(Q)$ and Γ (except for the ridge intensity to which only I was fitted, see below).

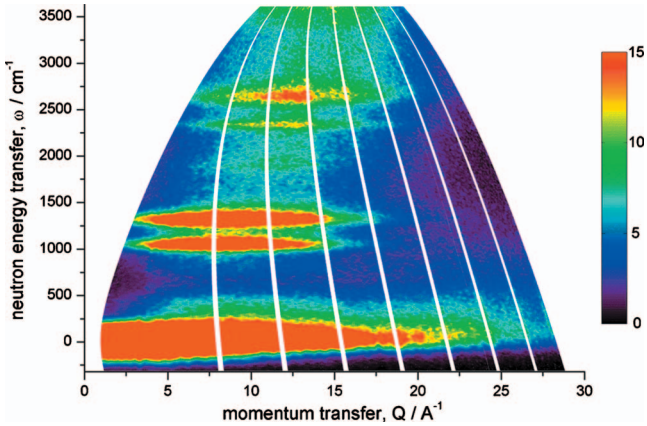

FIG. 3. The $S(Q,\omega)$ map of KH_2AsO_4 at 5 K, obtained on MARI, with an incident energy of 4087 cm^{-1}.

IV. EXPERIMENTAL

The KH_2AsO_4 was obtained from Apollo Scientific, Ltd., U.K., and used without further treatment. Two aluminum foil sachets of KHAs, one thick (7.35 g) and one thin (1.43 g, an approximately 3% scatterer), were held at ~5 K in the MARI spectrometer, The Science and Technology Facilities Council, The ISIS Facility, The Rutherford Appleton Laboratory, The Harwell Campus, OX11 0QX U.K. An incident neutron energy of 4087 cm^{-1} was used. The samples were in transmission geometry with the flat-plate at 45° to the beam. The detected time-of-flight neutron spectra were converted to the scattering law, $S(Q,\omega)$, by standard programs. This spectrometer and its data treatment programs are described in detail elsewhere.[16] The spectrum of the thin sample scaled linearly to match the spectrum of the thick sample, demonstrating that no significant artifacts were introduced into the spectrum of the thick sample by multiple scattering events. The same thick sample was also run on the TOSCA spectrometer, also at The ISIS Facility (see address above), at ~20 K, and again standard programs transformed the data to $S(Q,\omega)$. This spectrometer and its data treatment programs are described in detail elsewhere.[17]

V. DATA ANALYSIS

All of the analysis described below was undertaken on data obtained through the MSLICE suite of programs.[16] The results from MARI appear as a $S(Q,\omega)$ map, Fig. 3, and the energy transfer spectrum $S(\omega)$ is the sum of $S(Q,\omega)$ over all observed Q, Fig. 4. Cuts across the $S(Q,\omega)$ map, taken at constant ω, enable the Q-profile of the spectrum, at that ω, to be obtained. All of the cuts reported here were obtained by integrating the data in an 80 cm^{-1} wide strip, taken symmetrically about the central energy transfer of the cut. The detector coverage on MARI is incomplete and some scattering angles are unoccupied, therefore, the (Q,ω) map is discontinuous. Unfortunately these discontinuities introduce the appearance of structure into some extracted Q-profiles, usually on the high Q edge of the profiles. No attempt was made to correct for these effects, which were ignored. The Q-profiles were exported for further analysis in a commercial graphics package, "ORIGIN."[18]

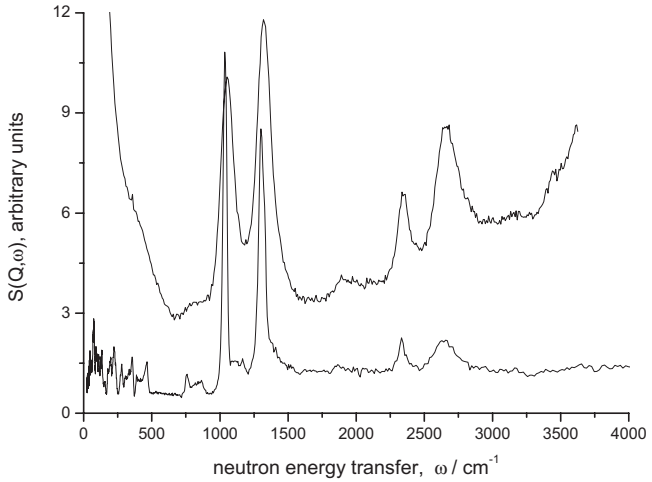

FIG. 4. The spectra of KH_2AsO_4. The upper trace, as derived from the $S(Q,\omega)$ data of Fig. 3 by summing across Q. The lower trace, as obtained from the TOSCA spectrometer, 20 K.

Using ORIGIN, flat backgrounds, estimated in the highest Q region, were subtracted from the Q-profiles. The corrected data gave good straight lines when fitted to either Eq. (8) (for one-quantum events), see Fig. 6(b), or Eq. (9) (for two-quantum events). However, if a straight line was obtained with Eq. (8), then the same data could not be well fitted to Eq. (9), and vice versa. The slopes of these lines are the best fitting α values and the y-intercepts are the best fitting φ factors; these values are reported in Table I.

VI. RESULTS

The $S(Q,\omega)$ map and the derived $S(\omega)$ spectrum of KHAs obtained on MARI are shown in Figs. 3 and 4, respectively. The INS spectrum of KHAs, as obtained on TOSCA, is also shown in Fig. 4 and detailed in Table II. The TOSCA spectrum is entirely in agreement with that published previously.[11] The TOSCA and MARI spectra of Fig. 4 differ in the presence of an extra feature in the MARI data at about 1900 cm^{-1}. The TOSCA spectrum is determined by its fixed trajectory across (Q,ω), that of MARI is obtained by integrating across all Q. Results at any given ω on MARI will contain data obtained at lower and higher Q than that obtained on TOSCA.[10] Here, it is the low Q data that allow us to distinguish the band at 1900 cm^{-1}. This is the first observation of this feature in the INS spectrum of KHAs. At the highest energy transfers the TOSCA spectrum is flat and unstructured but significant extra intensity is observed in this region on MARI. This extra intensity is an experimental artifact and comes from those neutrons that underwent several scattering events and almost stopped in the sample. This intensity was ignored.

A. The main features

The spectra consist of five clear transitions above 1000 cm^{-1} at 1036, 1307, 1900, 2335, and 2650 cm^{-1}. These can be compared to the assignments of the optical spectrum of KHAs (30 K): γ(OH)(0-1), δ(OH)(0-1) and the C, B, A bands at 1036, 1304, 1610, 2370, and 2700 cm^{-1}.[11,12] The lower energy bands are clearly in register and the higher energy bands are nearly so, but the 1900 and 1610 pair is not.

B. The ridge intensity

Following the theory outlined above, we have developed the intensity profiles, as a function of Q, at several energy transfers not associated with the transitions, see Fig. 5. We see from Fig. 3 that a ridge of intensity stretches from at least 1600 to 4000 cm^{-1} and all of the higher frequency INS features sit astride this ridge. Q-profiles of the ridge fitted to Eq. (10) as two-quantum events (at least in the limit that we cannot distinguish two-quantum from higher-quantum events, see above). Values of the α and φ parameters were extracted from I values alone and showed that φ is constant at 0.0025.

The α values, however, followed a specific trend. The positions in Q where the ridge reaches its maximum intensity move to higher values as the energy transfers, at which the profiles are taken, ω_P increase, such that

TABLE I. The fitting parameters obtained from fitting Eqs. (9) and (10) to the spectral features of KH_2AsO_4. The underlying intensity of the ridge has been subtracted, see text.

	Eq. (9)		Eq. (10)		FWHH[a]
Band position	φ	α	φ	β	Γ
cm^{-1}		$Å^2$		$Å^2$	80 cm^{-1}
1036	1.15	0.0162			1.20
1307	1.37	0.0136			1.44
1897	⋯	⋯	⋯	⋯	⋯
2335					
			0.0069	0.0141	1.94
Ridge corrected			0.0018	0.0145	1.11
2650					
			0.0172	0.0140	3.70
Ridge corrected			0.0050	0.0152	2.09
Average values		0.0149			

[a]As expressed in units of 80 cm^{-1}, the energy width used in generating the Q-profiles.

TABLE II. Showing the band positions, cm^{-1}, in potassium dihydrogen arsenate; as observed in the infrared, Raman, and INS techniques.

						INS, this work		
IR[a] 30 K	Raman[b] 7 K					MARI	TOSCA	Assignment
		$A_1(x,x)$	$A_1(z,z)$	A_2	B_1			
1050	1036					1050	1036	γ(OH)(0-1)
							1180	
	1298							
1300						1315	1307	δ(OH)(0-1)
	1329							
1610								ν(OH)onset
1780		1730	1660	1828	⋯			
						1900	⋯	γ(OH)(0-2)
1930		1922	1928	1940	⋯			
2370		2310	2256	2393	2344	2355	2335	γ(OH)(0-1)+δ(OH)(0-1)
2700		2655	2635	2660	2660	2645	2650	δ(OH)(0-2)

[a]Reference 11.
[b]Reference 12.

$$Q^2\alpha = 1 \quad \text{and} \quad \omega_P/16.71 = Q^2. \tag{11}$$

The ridge, therefore, follows a trajectory in (Q,ω) space that corresponds to the unit-mass oscillator line and is the same trajectory as that followed by TOSCA. That this ridge is of fixed intensity and effectively featureless, except for the two bands at 2335 and 2650 cm^{-1}, is clearly shown in the TOSCA spectrum, see Fig. 4.

C. *Q*-profiles

The *Q*-profiles of each transition are shown in Figs. 6(a)–6(d). Also shown in Fig. 6(b) is the fit of the 1307 cm^{-1} *Q*-profile to Eq. (10). To extract the *Q*-profile of the bands at 2335 and 2650 cm^{-1}, the intensity of the ridge profile was subtracted from the total profile. This is justified below. [The ridge intensity under the band was $\varphi=0.0025$, see above, and α is from Eq. (11).] From Fig. 6 we see that, while the 1036 and 1307 cm^{-1} *Q*-profiles are well described as those of fundamentals, the *Q*-profiles of 2335 and 2650 cm^{-1} are those for two-quantum events. The intensity remaining in the band at 1900 cm^{-1}, after subtracting the ridge intensity, was too small to give meaningful fits.

VII. DISCUSSION

As outlined in the Sec. I, the currently accepted interpretation of the optical features at about 2335 and 2650 cm^{-1} is that they arise from a single broad fundamental transition with a missing window of intensity. In this interpretation the intensity at 2335 and 2650 cm^{-1} comes from the ν(O–H) fundamental and the window is created by the δ(OH)(0-2) overtone; previous INS work has been interpreted in accordance with this model.[11] However, the *Q*-profiles of the bands at 2335 and 2650 cm^{-1} do not correspond to that of fundamentals but rather to those of two-quantum events. Moreover, their positions are clearly in line with expectations for the overtones and combinations of γ(OH)(0-1) and δ(OH)(0-1) oscillators with good mechanical harmonicity. We, therefore, assign the INS features at 2335 and 2650 cm^{-1} as the overtone and combination bands of the two fundamentals at 1036 and 1307 cm^{-1}, respectively. The simplest assignment of the remaining band at 1900 cm^{-1} would then be to an anharmonic overtone of the fundamental at 1036 cm^{-1} (harmonically expected at 2072 cm^{-1}, an anharmonicity constant x_e of 0.071 would bring it to 1900 cm^{-1}). These assignments are gathered together in Table II. From the work reported here, there is no evidence for Evans' holes in the region of 2200–2900 cm^{-1}.

Having rejected the previously held model for the interpretation of the distribution of intensities at higher energies it behoves us to attempt to provide an alternative. The MARI data clearly show that the 1307 cm^{-1} band is very close to being a harmonic unit-mass oscillator and we shall follow a simple harmonic approach. From the data in Table I, confirmed by the intensity ratios found in the TOSCA spectrum, we know that ${}^{\mathrm{Tr}}({}^{1036}\mathbf{B})/{}^{\mathrm{Tr}}({}^{1307}\mathbf{B})=0.84$. Immediately, however, we encounter a problem when we compare this ratio with other results from Table I; from Eqs. (4) and (5),

$$\frac{\mathrm{X3}\ {}^{\mathrm{Tr}}({}^{1307}\mathbf{B})^2}{30}\frac{15}{\mathrm{X}(0.84\,{}^{\mathrm{Tr}}({}^{1307}\mathbf{B}))\,{}^{\mathrm{Tr}}({}^{1307}\mathbf{B})} = \frac{{}^{2650}\varphi}{{}^{2335}\varphi} = 1.79,$$

but from observation,

$$\frac{{}^{2650}\varphi}{{}^{2335}\varphi} = \frac{0.0050}{0.0018} = 2.77.$$

Clearly, if we use the data from Table I to extract ${}^{\mathrm{Tr}}\mathbf{B}$ values directly they will be inconsistent. However, we can obtain the minimum value for ${}^{\mathrm{Tr}}({}^{1307}\mathbf{B})$, 0.0121 $Å^2$. This is remarkably close to its harmonic estimate 0.0128 $Å^2$ from Eq. (3), which is the maximum value that it can take. (Hence, ${}^{\mathrm{Tr}}({}^{1036}\mathbf{B})=0.0101=0.0121\times0.84$ $Å^2$.) So,

$$\mathbf{A}_{\mathrm{internal}}|_{\mathrm{min}} = \begin{bmatrix} 0.0101 & & \\ & 0.0121 & \\ & & {}^{\nu(\mathrm{OH})}\mathrm{B} \end{bmatrix}.$$

With these values we calculate ${}^{2335}\varphi$ and ${}^{2650}\varphi$ to be 0.0028 and 0.0050, respectively. When these are compared to the observed values, Table I, some 35% of the intensity at

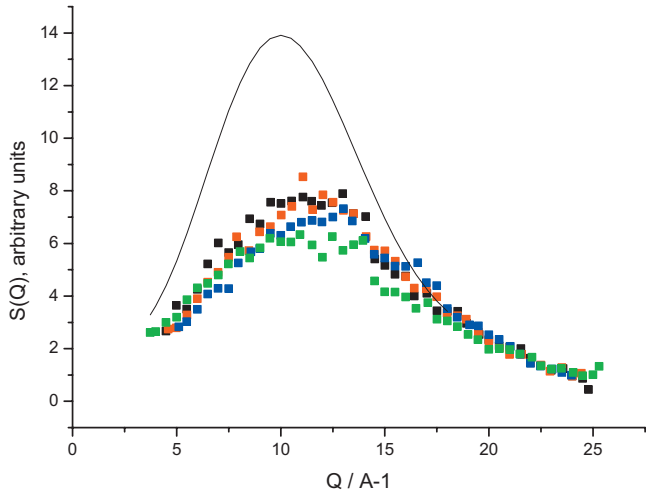

FIG. 5. Q-profiles of the ridge intensity at $\omega=1690$ cm^{-1}, in green; $\omega=1906$ cm^{-1}, in black; $\omega=1968$ cm^{-1}, in red; $\omega=2200$ cm^{-1}, in blue. Also shown, black line, is the Q-profile of the 2650 cm^{-1} band.

2335 cm^{-1} is seen to be missing. In the context of hydrogen bonding it would not be unusual to invoke a resonance process to account for this missing intensity and this would also provide a ready explanation for the weakness of the feature at 1900 cm^{-1}; it lies even closer in energy to the resonance. We have extrapolated linearly back to estimate the position of a putative transition at which all intensity would be lost; that value was 1750 cm^{-1}. We shall return to this topic below; but for now we arbitrarily associate 1750 cm^{-1} with ν(O–H) and so obtain a harmonic estimate for the final element in $\mathbf{A}_{\mathrm{Int}}$, ${}^{\mathrm{Tr}}({}^{\nu(\mathrm{O-H})}\mathbf{B})=0.0096$ Å^2.

Recalling Eqs. (6) and (7) and using the observed α values, Table I, we obtain an estimate of $\mathbf{A}_{\mathrm{tot}}$ by trial and error,

$$\mathbf{A}_{\mathrm{tot}}=\begin{bmatrix}0.0186 & & \\ & 0.0121 & \\ & & 0.0131\end{bmatrix} \text{ yielding } \begin{matrix}\alpha^{1036}=0.0162\\ \alpha^{1307}=0.0136\end{matrix}.$$

The average of the observed α values, Table I, approximates to ${}^{\mathrm{Tr}}\mathbf{A}/3(=0.0146$ Å$^2)$ as it should. Unfortunately, there are no crystallographic ${}^{\mathrm{Tr}}\mathbf{U}$ values for the hydrogen atom in KHAs for us to compare directly with our ${}^{\mathrm{Tr}}\mathbf{A}_{\mathrm{tot}}$, 0.0438 Å^2. However, as presented above, we may use ${}^{\mathrm{Tr}}\mathbf{A}={}^{\mathrm{Tr}}\mathbf{U}(\mathrm{H})\approx 0.054\,42$ Å^2 for comparison. Considering the limitations implicit in this comparison we may conclude that our estimate of $\mathbf{A}_{\mathrm{tot}}$ would probably be confirmed by a neutron diffraction experiment.

We have also attempted to extract the component values for $\mathbf{A}_{\mathrm{tot}}$ under the assumption that the ridge is not an independent spectral feature; here the ridge would be seen as produced from a series of overlapping, more or less broad, bands. Under these circumstances, values for the uncorrected φ parameters, see Table I, were obtained from the unsubtracted data. These unsubtracted data lead to very large values for ${}^{\mathrm{Tr}}({}^{1036}\mathbf{B})$ and ${}^{\mathrm{Tr}}({}^{1307}\mathbf{B})$ (0.042 and 0.049 Å^2, respectively, and give a minimum value for ${}^{\mathrm{Tr}}\mathbf{A}_{\mathrm{tot}}=0.092$ Å^2). These values are thus inconsistent with both the 0.054 42 Å^2 estimate and the approximate ${}^{\mathrm{Tr}}\mathbf{A}/3$ value given above. We conclude that the ridge is best regarded as an independent spectral feature upon which sit the bands at 2335 and 2650 cm^{-1}.

We interpret the ridge intensity as the pseudorecoil of the hydrogen atom in the H-bond. Above a certain energy, the onset, the shape of the ν(O–H) potential broadens, allowing the hydrogen atom to explore a greater volume of space than it would if confined in a harmonic well. All ν(O–H) excitations above onset lead to a constant scattering intensity that follows the hydrogen recoil line and has the Q-profile of a multiquantum excitation.[19] Hydrogen recoil has been observed previously on TOSCA and MARI.[20] Recoil scattering should demonstrate a broadening with Q but our data were taken over too narrow a range in Q to exploit this test effectively.[19]

Above, we estimated the onset energy to be about 1750 cm^{-1} and arbitrarily assigned this value to ν(O–H). This is unreasonable since it dissociates ν(O–H) from any spectral feature. We believe that the broad optical C feature about 1610 cm^{-1} (Ref. 11) would make a good candidate for ν(O–H). Moreover, this assignment would produce only a slightly different harmonic value for ${}^{\mathrm{Tr}}({}^{\nu(\mathrm{O-H})}\mathbf{B})$, now 0.0104 Å^2, and make no difference to the arguments we advance above.

We have explored the resonance interactions between ν(O–H) and the other vibrations; as expected the closer the feature is to 1610 cm^{-1} the greater the loss of spectral intensity. Based on the harmonic model presented above, the band at 1900 cm^{-1} has probably lost some 95% of its intensity (although the very weakness of the feature makes it difficult to provide a better estimate) and the intensity loss in the 2335 cm^{-1} band is 35%. In the Appendix we outline a Fermi-resonance view of these losses; the results correspond to coupling matrix-elements of about 145 and 360 cm^{-1} for the 1900 and 2335 cm^{-1} bands, respectively [with some modest variation in these values, if the ν(O–H) assignment lies elsewhere than at 1610 cm^{-1} but still in the region 1500–1800 cm^{-1}]. The changes to the band positions, imposed by Fermi-resonance, fall within the energy FWHH we observe and have no impact on the assignment scheme we propose.

We believe that the optical spectra are best regarded as the result of strong electrical anharmonicity in the system. The ν(O–H) ridge is a continuum from about 1610 cm^{-1}, which interacts strongly with those modes retaining significant hydrogen atom displacement, δ(OH)(0-2) and γ(OH) $\times$(0-1)+δ(OH)(0-1). The normally weak optical transitions associated with these modes are thus strongly enhanced but the γ(OH)(0-2), which retains very little hydrogen atom displacement, remains weak both optically and in the INS.

Although this work has focused on the specific example of potassium dihydrogen arsenate it has demonstrated how INS can be used to further understand the spectral features observed in molecular systems exhibiting significant hydrogen bond interactions. The INS data complement and enhance spectral information obtained more routinely by optical techniques, especially infrared spectroscopy. It should now be possible to extend this appreciation within molecular systems to the more challenging domain of surface chemistry

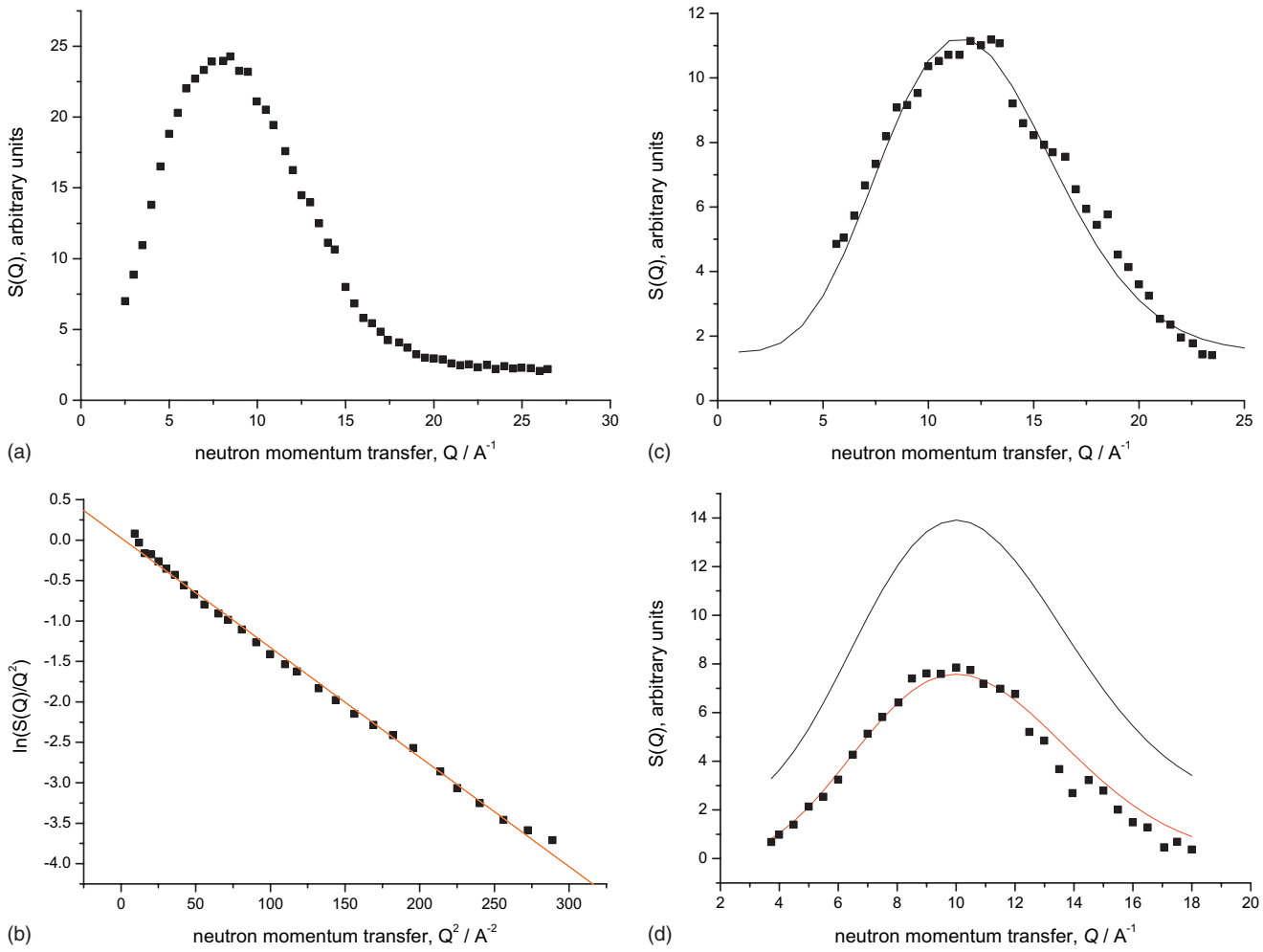

FIG. 6. Q-profiles of the transitions at (a) ω=1036 cm^{-1}; (b) ω=1307 cm^{-1} [fitted to Eq. (10), red line]; (c) ω=2335 cm^{-1} [corrected intensity with best fitting two-quantum curve, Eq. (5)]; (d) ω=2650 cm^{-1} [uncorrected intensity, black line; corrected intensity, data points; best fitting two-quantum curve, red line, Eq. (4)]. See text.

and heterogeneous catalysis, with the role of surface hydroxyl groups representing an ideal point of departure.

VIII. CONCLUSIONS

Using INS spectroscopy we have studied the ν(O–H) region of a known "A, B, C" hydrogen bonded system, potassium dihydrogen arsenate. The broad spectral feature observed in infrared spectroscopy is shown to be associated with a ridge of constant intensity in the INS, which follows the recoil line for a unit-mass particle. The onset energy of the ridge is unclear but, we believe, is associated with the optical "C" feature at 1610 cm^{-1}, and which we assign to ν(O–H). The "B" and "A" optical bands were both demonstrated to be two-quantum events and are, thus, not associated with the fundamental ν(O–H). Rather they are the overtone band δ(OH)(0-2) and the combination band γ(OH) $\times$(0-1)+δ(OH)(0-1), which both sit astride the ridge and there is no evidence for Evans' holes. The other overtone, γ(OH)(0-2), has been assigned to a very weak INS feature, observed for the first time in this work, at 1900 cm^{-1}. Starting from a simple harmonic model it was shown that intensity could be lost from the γ(OH) overtone and combination bands through Fermi-resonance. The elements of the **A** and **B** tensors of the assumed harmonic hydrogen vibrations were extracted.

ACKNOWLEDGMENTS

Here we should like to thank the Science and Technology Facilities Council for access to the ISIS neutron beams and Dr. J. Taylor for his experimental assistance.

APPENDIX: FERMI-RESONANCE

The effects of Fermi-resonance on neutron spectra have been detailed previously and are best treated in the incoherent approach.[21] Then, using the γ(OH)(0-2) resonance as an example, the intensity redistribution in the Fermi doublet ν(O–H)–γ(OH)(0-2) at 1610 and 1900 cm^{-1} is according to

$$S(Q,\omega)_{1610} = a^2 S(Q,\omega)_{\nu(\mathrm{OH})} + 2ab\sqrt{S(Q,\omega)_{\nu(\mathrm{OH})}}\sqrt{S(Q,\omega)_{2\gamma(\mathrm{OH})}} + b^2 S(Q,\omega)_{2\gamma(\mathrm{OH})},$$

$$S(Q,\omega)_{1900} = b^2 S(Q,\omega)_{\nu(\mathrm{OH})} - 2ab\sqrt{S(Q,\omega)_{\nu(\mathrm{OH})}}\sqrt{S(Q,\omega)_{2\gamma(\mathrm{OH})}} + a^2 S(Q,\omega)_{2\gamma(\mathrm{OH})},$$

where

$$a = \sqrt{\left(\frac{\Delta+\delta}{2\Delta}\right)} \quad b = \sqrt{\left(\frac{\Delta-\delta}{2\Delta}\right)}$$

and

$$\delta = (\omega^{\mathrm{unperturbed}}_{2\gamma(\mathrm{OH})} - \omega^{\mathrm{unperturbed}}_{\nu(\mathrm{OH})}),$$

with

$$1900 = \frac{(\omega^{\mathrm{unperturbed}}_{\nu(\mathrm{OH})} + \omega^{\mathrm{unperturbed}}_{2\gamma(\mathrm{OH})})}{2} + \frac{\Delta}{2},$$

$$1610 = \frac{(\omega^{\mathrm{unperturbed}}_{\nu(\mathrm{OH})} + \omega^{\mathrm{unperturbed}}_{2\gamma(\mathrm{OH})})}{2} - \frac{\Delta}{2}.$$

In the absence of Fermi-resonance the spectral features would have appeared at their $\omega^{\mathrm{unperturbed}}$ values. Since the observed intensity $S(Q,\omega)_{1610}$ contains contributions from both $S(Q,\omega)_{2\gamma(\mathrm{OH})}$ and $S(Q,\omega)\gamma_{(\mathrm{OH})+\delta(\mathrm{OH})}$, the a and b values for this doublet are best estimated from the $S(Q,\omega)_{1900}$ intensity.

[1] G. Gilli and P. Gilli, J. Mol. Struct. **552**, 1 (2000).
[2] J. Dreyer, J. Chem. Phys. **127**, 054309 (2007).
[3] M. F. Claydon and N. Sheppard, Journal of the Chemical Society D: Chemical Communications **23**, 1431 (1969).
[4] J. E. Bertie and J. P. Devlin, J. Chem. Phys. **79**, 2092 (1983) and references therein.
[5] A. G. Pelmenschikov, J. H. M. C. van Wolput, J. Jänchen, and R. A. van Santen, J. Phys. Chem. **99**, 3612 (1995).
[6] L. Kubelková, J. Kotrla, and J. Florián, J. Phys. Chem. **99**, 10285 (1995).
[7] A. R. McInroy, D. T. Lundie, J. M. Winfield, C. Dudman, P. Jones, S. F. Parker, J. W. Taylor, and D. Lennon, Phys. Chem. Chem. Phys. **7**, 3093 (2005).
[8] J. Tomkinson, Spectrochim. Acta, Part A **48**, 329 (1992).
[9] A. R. McInroy, D. T. Lundie, J. M. Winfield, C. C. Dudman, P. Jones, S. F. Parker, and D. Lennon, Catal. Today **114**, 403 (2006).
[10] P. C. H. Mitchell, S. F. Parker, A. J. Ramirez-Cuesta, and J. Tomkinson, *Vibrational Spectroscopy with Neutrons* (World Scientific, Singapore, 2005).
[11] N. Le Calvé, B. Pasquier, and Z. Ouafik, Chem. Phys. **222**, 299 (1997).
[12] E. V. Chisler and V. Y. Davydov, J. Mol. Struct. **177**, 231 (1988).
[13] M. Ichikawa, D. Amasaki, T. Gustafsson, and I. Olaovsson, J. Phys. Soc. Jpn. **70**, 2327 (2001).
[14] J. D. Dunitz, *X-Ray Analysis and the Structure of Organic Molecules* (VCH, Basel, 1995).
[15] R. J. Nelmes, Z. Tun, and W. F. Kuhs, Ferroelectrics **71**, 125 (1987).
[16] M. Arai, A. D. Taylor, S. M. Bennington, and Z. A. Bowden, *Recent Developments in the Physics of Fluids*, edited by W. S. Howells and A. K. Soper (Hilger, Bristol, 1992), pp. F321–F328.
[17] D. Colognesi, M. Celli, F. Cilloco, R. J. Newport, S. F. Parker, V. Rossi-Albertini, F. Sacchetti, J. Tomkinson, and M. Zoppi, Appl. Phys. A: Mater. Sci. Process. **74**, s64–s66 (2002).
[18] see: http://www.OriginLab.com.
[19] J. Mayers, C. Andreani, and G. Baciocco, Phys. Rev. B **39**, 2022 (1989).
[20] F. Fillaux, R. Papoular, S. M. Bennington, and J. Tomkinson, J. Non-Cryst. Solids **188**, 161 (1995).
[21] C. V. Berney, J. Chem. Phys. **62**, 936 (1975).